Preliminary results on the simulation of the 1999 Orissa supercyclone using a GCM with a new boundary layer code

T. N. Venkatesh, Vidyadhar Mudkavi, S. Rajalakshmy, V. R. Sarasamma, U. N. Sinha and R. Narasimha*

National Aerospace Laboratories, Bangalore
*Jawaharlal Nehru Centre for Advanced Scientific Research, Bangalore

November 10, 2005

Abstract

We present here preliminary results from the simulation of the Orissa supercyclone using a new AGCM code (named Varsha) written as part of a NMITLI project. The simulation is initialized at 00 UTC, 26 October 1999, using ECMWF T-106 initial conditions. The control run is made using the Varsha code at a T-80 resolution with a standard Monin-Obukhov boundary layer code incorporating a gustiness factor. With the horizontal resolution improved to 120 spectral modes with a 78 km grid spacing, and a new boundary layer parameterization at low winds, the code shows substantial improvements: the maximum error is reduced from 350 to 234 km at 36 h after initialization, 310 to 34 km at 48 h, and 410 to 55 km at 96 h. It is suggested that part of the explanation for this improvement lies in the improved estimation of surface forces and torque in the new boundary layer code. The role of torque is particularly interesting as the major contribution to it comes from the outer regions of the cyclone where the winds are relatively low but the area on which the surface force acts and its moment arm are both high. Intriguingly the higher surface forces arise also from the higher winds predicted by the new code. An interesting finding is that, on both track and minimum pressure, the improvement due to higher resolution is greater with the new boundary layer module. Further analysis is necessary to assess the effect of other eddy fluxes (sensible heat, moisture) on cyclone track prediction.

1 Introduction

Accurate simulation of cyclone tracks is a continuing challenge in the field of numerical weather prediction. A wide range of numerical models - from global GCMs to specialized mesoscale codes (MM5) - are now used worldwide for this purpose. Although the accuracy

of these models has improved over the years and is now considerably better than that of statistical models such as CLIPER (Gross, 2000) , the errors are still too large and the need persists for greater accuracy.

For India, tropical cyclones (TC) in the Bay of Bengal are the more dangerous as compared to those in the Arabian Sea. This is because (i) more TCs form in the Bay of Bengal due to its higher surface temperature, and (ii) the predominantly northwestward propagation of these systems means that landfall over India occurs more often for Bay of Bengal cyclones. One of the most destructive in recent times was the Orissa supercyclone of 1999. This has been a good test case for checking current simulation capabilities as the initial conditions obtained from global datasets (from NCEP or ECMWF) are reasonably accurate due to the large size of the system.

Emanuel (1999) has emphasized the important role of surface fluxes in cyclone prediction. In most numerical models, the surface layer is computed using the Monin-Obukhov scaling relations. In addition, gustiness factors are often in use (Hack et al, 1993). Since convection in the tropics often occurs at low winds, it has been suggested by Rao and Narasimha (2005) that a different scaling, appropriate to what they have called 'weakly forced convection', be used in this regime. These ideas were incorporated into the AGCM Varsha 1.0 (Sinha et al, 2005 b) as part of the NMITLI project, and tested for the Orissa supercyclone. This resulted in significant improvements in the predicted cyclone track. This paper is a preliminary report on the performance of Varsha 1.0 on predicting the Orissa supercyclone, and a brief analysis of how the new boundary layer scheme might have led to the observed improvements in the simulations reported herein.

2 AGCM Varsha

All the simulations carried out in this study employ the Varsha GCM code version 1.0. This is a hydrostatic spectral general circulation model which has its roots in the NCMRWF's GCM T-80 code which was parallelized by NAL in 1993 (Sinha et al, 1994). It was subsequently re-engineered using FORTRAN 90 (Nanjundiah and Sinha, 1999) and, as part of the NMITLI project, new radiation and boundary layer modules were added (Sinha et al, 2005 a) . The model can be run at different spectral truncation as well as physical grid resolutions. The number of vertical layers is 18 and the physical parameterizations include the Kuo-Anthes cumulus scheme and Alpert gravity wave drag parameterization. The shortwave radiation is computed as described in Sinha et al (1994) , while there are two options for the long wave radiation computation: (i) The Fels-Schwarzkoff scheme and (ii) a new scheme devised for Varsha based on Varghese et al (2003). For the boundary layer the options are (i) the Monin-Obukhov scaling along with a gustiness parameter, and (ii) a new boundary layer scheme based on the scaling arguments of Rao and Narasimha (2005) which will be described in the next section. In this paper, results using the Fels-Schwarzkoff long wave radiation scheme and the two boundary layer schemes are presented.

3 Scaling appropriate for weakly forced convection

We first describe the basis for the present boundary layer code. Analysis of atmospheric observational data (Rao and Narasimha, 2005) from MONTBLEX and BLX83 was found to indicate that the conventionally defined drag and heat transfer coefficients increase rapidly as wind speed falls. It was shown that, at low winds,

1. there is a linear increase of drag with wind speed and
2. the observed heat flux is independent of wind speed.

These findings are not consistent with the so-called free-convection limit of Monin-Obukhov theory. They are instead best seen as the result of a new regime of weakly forced convection, in which the heat flux is determined solely by temperature differentials as in free convection, and the momentum flux by a perturbation linear in wind on free convection. This regime is governed by a new velocity scale determined by the heat flux (rather than by the friction velocity as in classical turbulent boundary layer theory). Novel definitions of the drag and heat exchange coefficients, based on appropriate heat-flux velocity scales, are found to be independent of wind speed at low winds.

The new boundary layer scheme uses these results in the following way. A matching velocity V_m, which is a measure of the maximum velocity upto which the low wind regime is valid, is first defined. If the lowest model level wind (V) is above V_m for an atmospheric column, the standard Monin-Obukhov scaling is used. If V is below V_m, the low wind regime scaling is used. The fluxes are matched at V_m. Although the value of V_m may be found from the heat flux scaling arguments of Rao and Narasimha (2005), it suffices here to determine V_m by trial. The main reason for adopting this procedure is that the wind at first sigma level in the model cannot directly replace the wind at 10 m used in the analysis of Rao and Narasimha (2005).

4 Results and discussion

Simulation of the Orissa supercyclone was carried out using initial conditions obtained from ECMWF, available at T-106 resolution. Five day integrations were performed on the global resolution starting from 00 UTC of 26 October 1999. Results are presented for two different resolutions, both with the old boundary layer module (called 'control' below) and the 'present' code with different values of V_m. The two resolutions are: (i) 80 mode, 256×128 grid and (ii) 120 mode, 512×256 grid.

4.1 Simulated tracks

Figure 1 shows track simulations at the two resolutions. The effect of resolution can be clearly seen. The higher resolution improves the track considerably. Table 1 gives a comparison

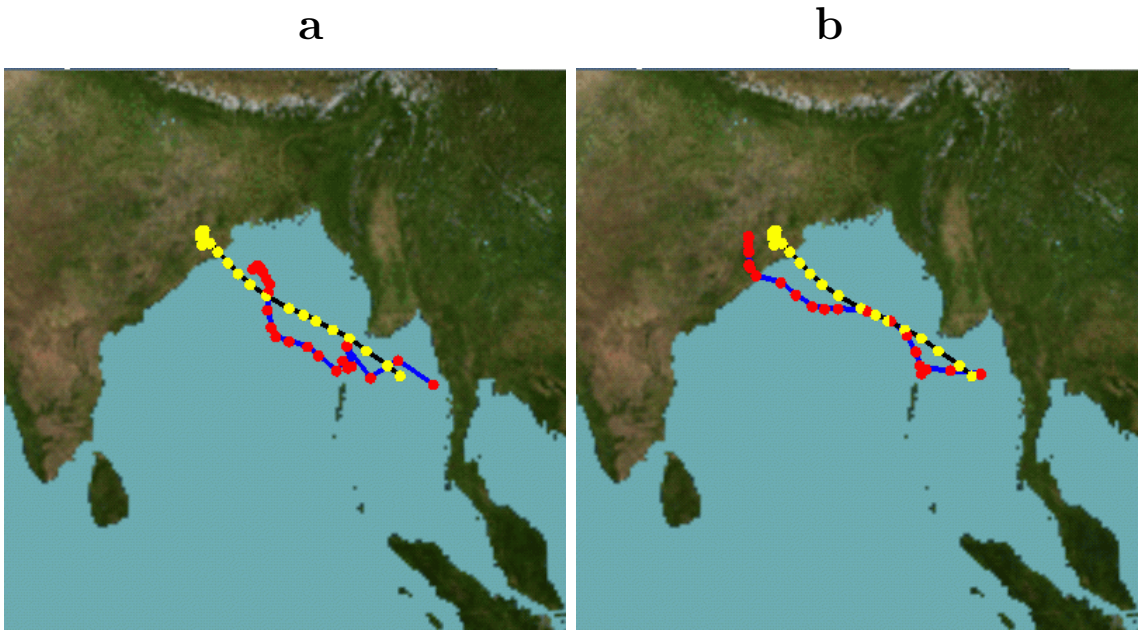

Figure 1: Computed tracks with (a) 80 modes and (b) 120 modes, with earlier boundary layer module.

between the best forecast (with the new boundary layer and higher resolution) and the best track as per the IMD data. It may be noted that the initial position of the cyclone in the ECMWF analysis differed from the IMD position by around 80 km.

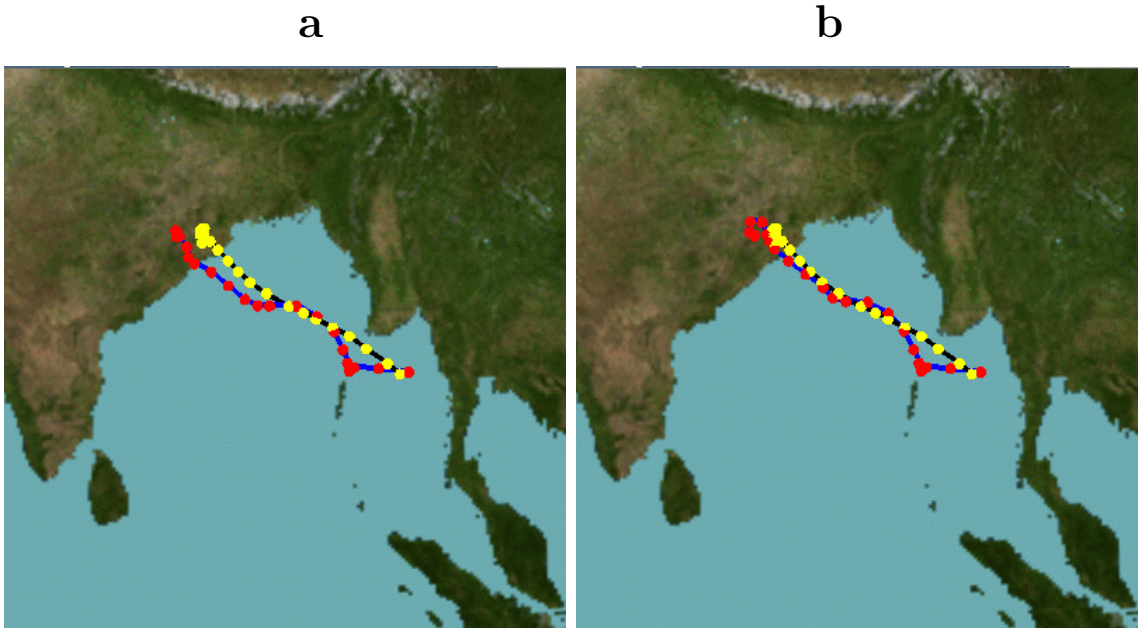

Figure 2: Computed tracks with 120 modes using the new boundary layer scheme with a matching velocity of (a) 3 m/s and (b) 5 m/s.

The effect of the present boundary layer module can be seen from figure 2. For $V_m = 3$ m/s the simulated track is closer to the observed one, and for $V_m = 5$ m/s the trajectory is very good and the landfall point accurate.

The storm made landfall by 29 October 03 UTC. But, it retained severe cyclonic intensity for another 24 hours. In observations, it had remained almost stationary till 30 October 00 UTC. As seen in figure 2b, in the simulation too, the storm remained almost stationary after landfall for nearly 24 hours.

4.2 Track errors

Track errors as a function of time are shown in figure 3. (The reference ('observed') track is the "best track" data provided by IMD)

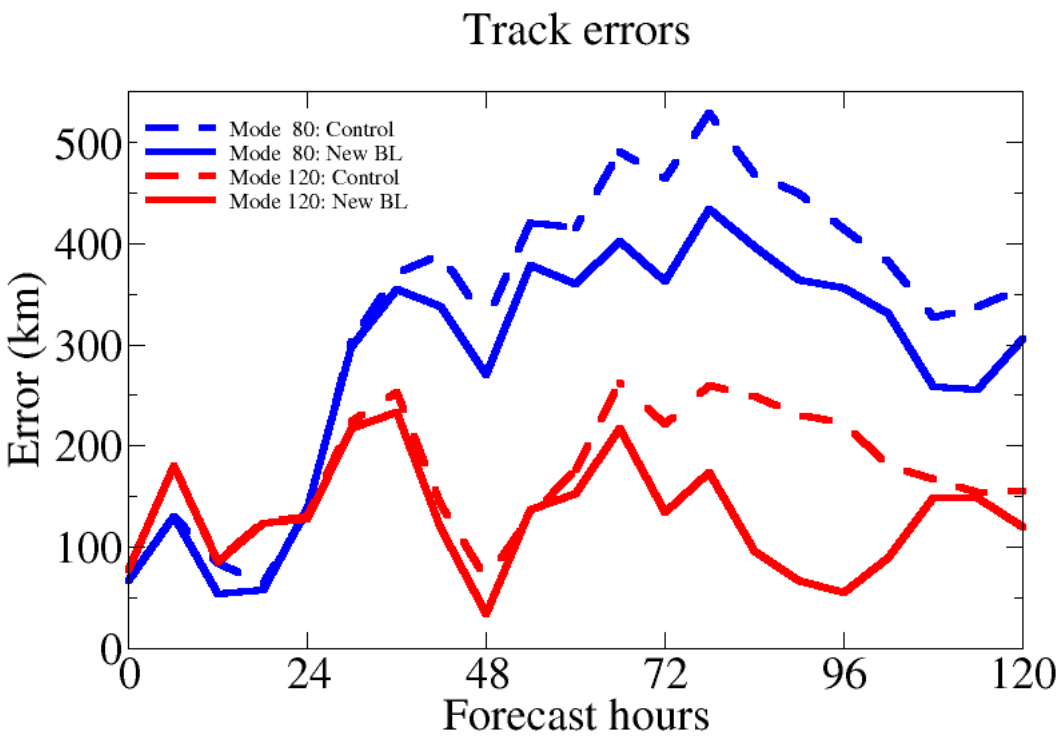

Figure 3: Plot of vector track errors (km) as a function of time between the observed best track data positions (IMD) and predicted positions. The curves corresponding to the control run are shown by dashed lines and for new boundary layer with V_m of 5 m/s by full lines. The 80 mode results are coloured blue and the 120 mode results are coloured red.

The effect of the resolution is to reduce the track error by a maximum of nearly 300 km at $t = 48$ h. The present boundary layer scheme further improves the track by about 100 km at T-80 resolution and by 270 km at T-120 resolution. The effect is most prominent between 60 h and 108 h. It is interesting to note that the track error is minimum (about 34 km) at $t = 48$ h.

Table 1: Comparison of the position and central pressure of the cyclone between the observed IMD best estimates and predicted ones.

	IMD data			Predicted data			Errors	
Date and time (UTC)	Lon (E)	Lat (N)	Central pressure (hPa)	Lon (E)	Lat (N)	Central pressure (hPa)	Vector error in position (km)	Difference in central pressure (hPa)
2600	96.5	13.5	1002	95.9	13.9	1003	77	-1
2606	96.0	13.5	1002	94.5	14.1	1002	180	0
2612	94.0	14.5	998	93.3	14.2	1004	85	-6
2618	93.5	15.0	998	93.1	14.0	1001	123	-3
2700	93.0	15.5	998	93.0	14.4	992	127	+6
2706	91.5	16.5	992	92.7	15.0	993	216	-1
2712	90.5	17.0	992	92.3	15.8	992	234	0
2718	90.5	17.0	986	91.6	16.7	994	119	2
2800	90.5	17.5	986	90.6	17.2	993	34	3
2806	88.5	18.0	968	89.4	17.2	990	136	-22
2812	88.0	18.5	940	88.9	17.4	988	153	-48
2818	87.0	19.3	912	88.4	17.8	990	217	-78
2900	87.0	19.6	912	87.6	18.5	988	134	-76
2906	86.0	20.5	912	86.7	19.0	991	174	-78
2912	86.0	20.5	N/A	86.0	19.6	988	97	
2918	86.0	20.5	N/A	85.8	19.9	989	67	
3000	86.0	20.5	N/A	85.6	20.2	992	55	
3006	86.0	20.5	N/A	85.3	20.7	994	89	
3012	86.0	20.5	N/A	84.7	20.8	994	148	
3018	86.0	20.5	N/A	84.4	20.3	996	149	
3100	86.0	20.5	N/A	84.9	20.2	996	120	

4.3 Role played by the BL on track prediction

To understand the role played by the new BL scheme, the surface winds (i. e. at the lowest model level of 995 mb) from the higher resolution run are plotted in figure 4. To indicate the region of low winds (where the new boundary layer scaling is effective), a blue contour at wind level of 5 m/s is drawn. It is seen that, in general, the effect of the present boundary layer code is to make the cyclone more compact, and hasten landfall. Furthermore, it will be seen that the winds predicted by the new code are generally higher; the differences being most marked in figures 4a and 4b (48 h, 72 h respectively after initialization).

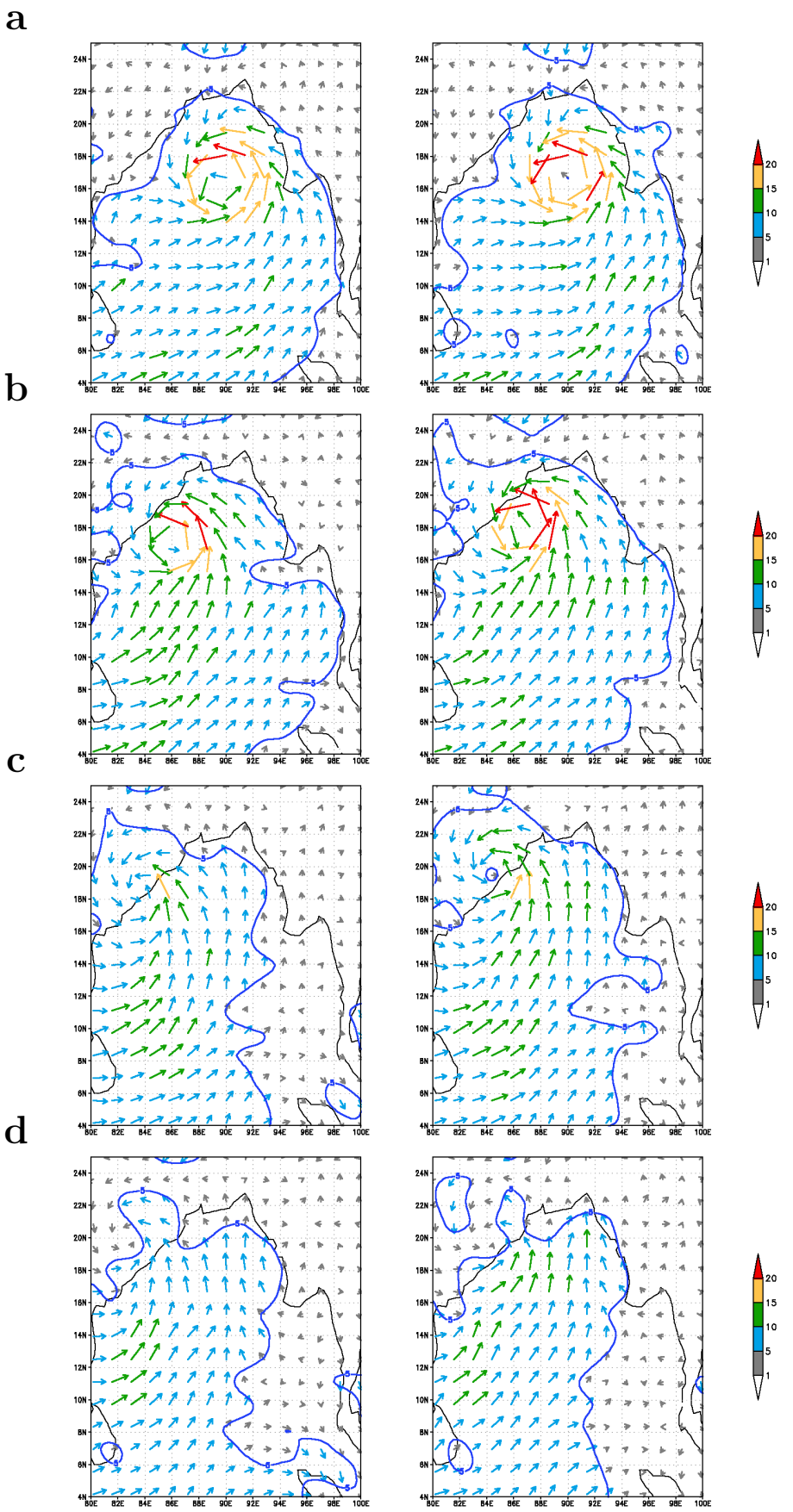

Figure 4: Model surface winds (m/s) after (a) 48 h, (b) 72 h, (c) 96 h and (d) 120 h of integration. Left panel: Control and right panel: New BL with $V_m = 5$ m/s. Blue contour is at surface wind value of 5 m/s.

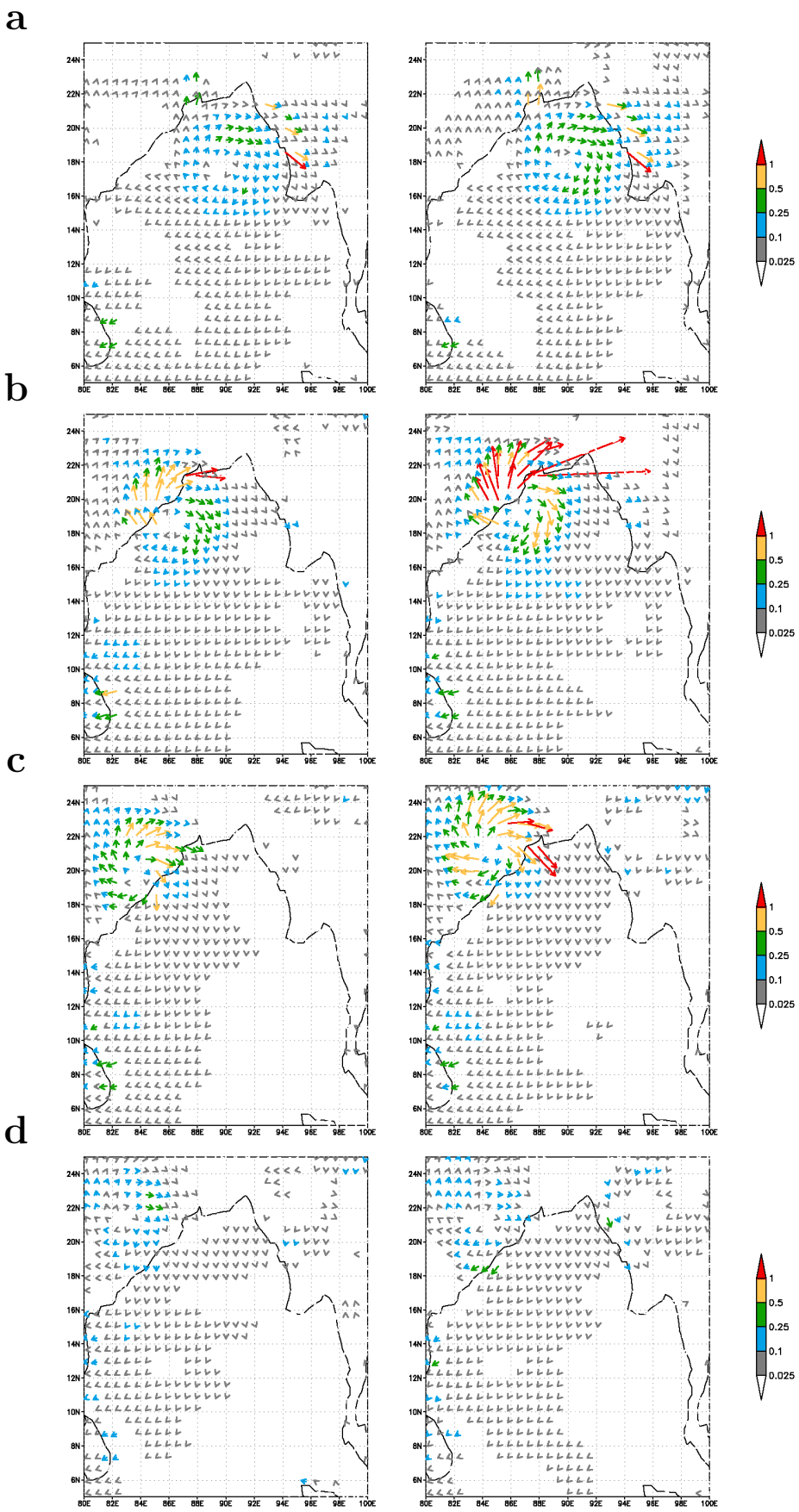

Figure 5: Surface stress fields (N/m^2) after (a) 48 h, (b) 72 h, (c) 96 h and (d) 120 h of integration. Left panel: Control; Right panel: New BL with $V_m = 5$ m/s

To analyze possible reasons for these features, the surface stresses calculated from the boundary layer module are plotted in figure 5. Here the stress $\boldsymbol{\tau}$ is computed as

$$\boldsymbol{\tau} = -C_D \frac{1}{2} \rho V^2 \mathbf{n} \tag{1}$$

by the new boundary layer module. Here, C_D is the drag coefficient, ρ the density, $\mathbf{n}$ is the unit vector along the wind direction and V the wind speed at lowest model level. C_D varies at each grid point and is computed by the boundary layer module.

Interestingly, the new code predicts much higher surface stresses, especially near the centre of the cyclone; the differences are dramatic in figures 5b and 5c (72 h and 96 h after initialization). These higher stresses are related to the higher winds predicted by the new code, as seen in figures 4a and 4b.

The total surface force acting on the cyclone is calculated as

$$\mathbf{F}_{surf} = \int \boldsymbol{\tau} dx\, dy \tag{2}$$

where $\boldsymbol{\tau}$ is the stress vector, and the integration is carried out over a circle of radius r_c around the centre of the cyclone. The value of r_c is fixed at 640 km. This radius is sufficient to cover the entire circulation of the cyclone. Results are presented in Figure 6 (note that the figure presents the surface force acting on the atmosphere, i. e., it is opposite in direction to the drag acting on the surface). It is seen that the surface force $\mathbf{F}_{surf}$ is generally higher with the new BL code, being about $2\frac{1}{2}$ times as large at 72 h. Directions are also different, especially just before and immediately after landfall, possibly accounting for the remarkable change in cyclone track that is noticed around that time.

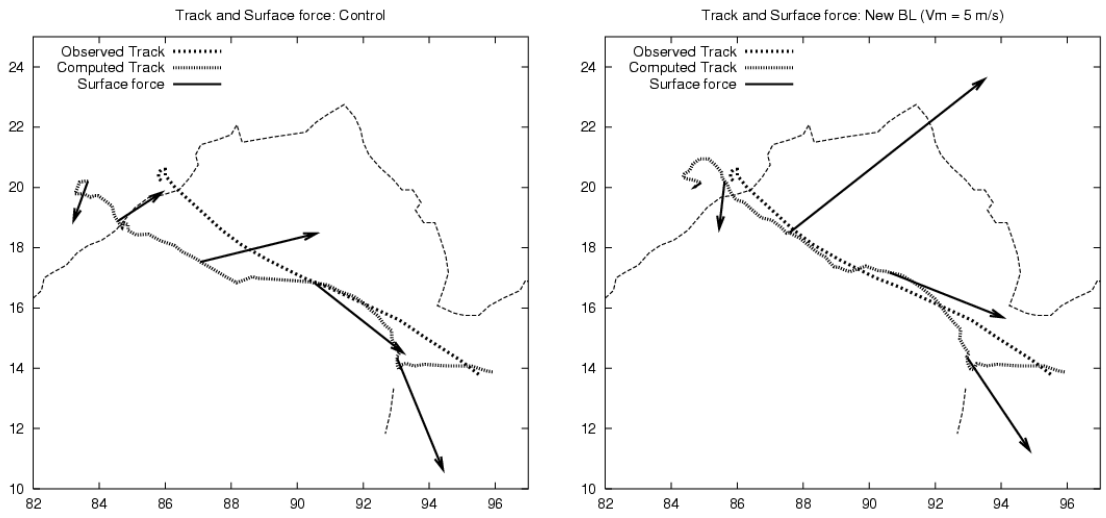

Figure 6: Net surface force due to the surface layer stresses at 24 h intervals along the cyclone tracks. Left panel: Control. Right panel: New BL with $V_m = 5$ m/s

We also compute the radial distribution of the torque density, defined as

$$T(r) = \left| \int_0^{2\pi} \hat{\mathbf{r}} \times \boldsymbol{\tau} r^2 d\theta \right| \tag{3}$$

where $\hat{\mathbf{r}}$ is unit vector along the radius and θ is the polar angle. The total torque is given by

$$T_{total} = \int_0^{r_c} T(r)dr \tag{4}$$

The radial distributions of torque are shown in Figure 7, along with the radial distributions of circumferentially averaged wind speed. Here, the non-dimensional distance $r^* = r/\Delta x$, where Δx is the grid spacing.

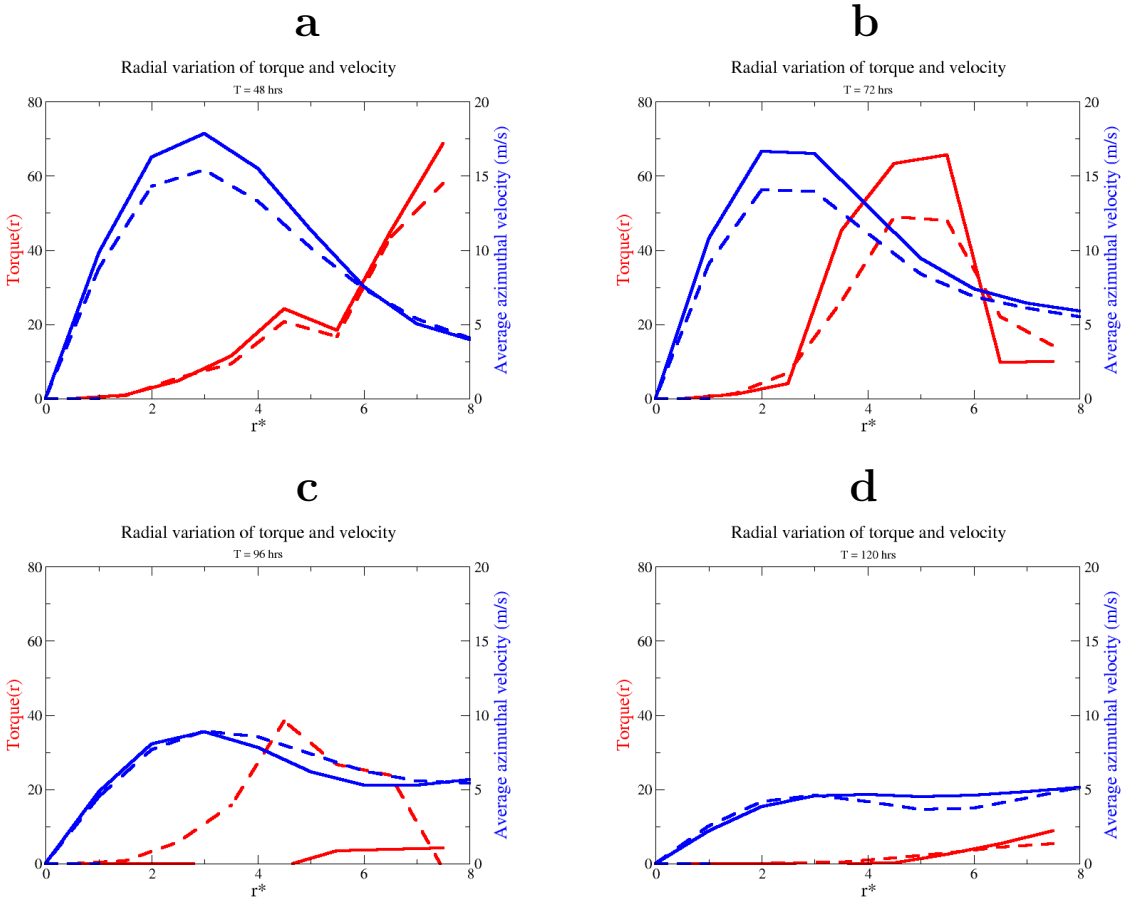

Figure 7: Comparison of the radial variation of torque (red line, scaled units) and azimuthal velocity (blue lines) on the cyclone at (a) 48 h, (b) 72 h, (c) 96 h and (d) 120 h. The control run results are represented by dashed lines and the new BL results by full lines.

It is seen that at 72 h the new code gives a surface torque that is about 50-200 % higher at $r^* \geq 4.5$; the largest differences come from the low-wind regions. At 96 h, on the other hand, the torque from the new code is less when compared with the standard boundary layer code. It must be remembered that when the circumferentially averaged wind speed is close to 5 m/s, there will be areas where the local wind falls below 5 m/s.

The variation of total torque with time is shown in figure 8. From initialization upto 72 h, the total torque due to the new code is higher by about 25 %. In the new code, the torque peaks at 72 h and quickly reduces to a low value. The higher torque (before 72 h) may be responsible for spinning up the cyclone more effectively, thereby making it tighter and stronger.

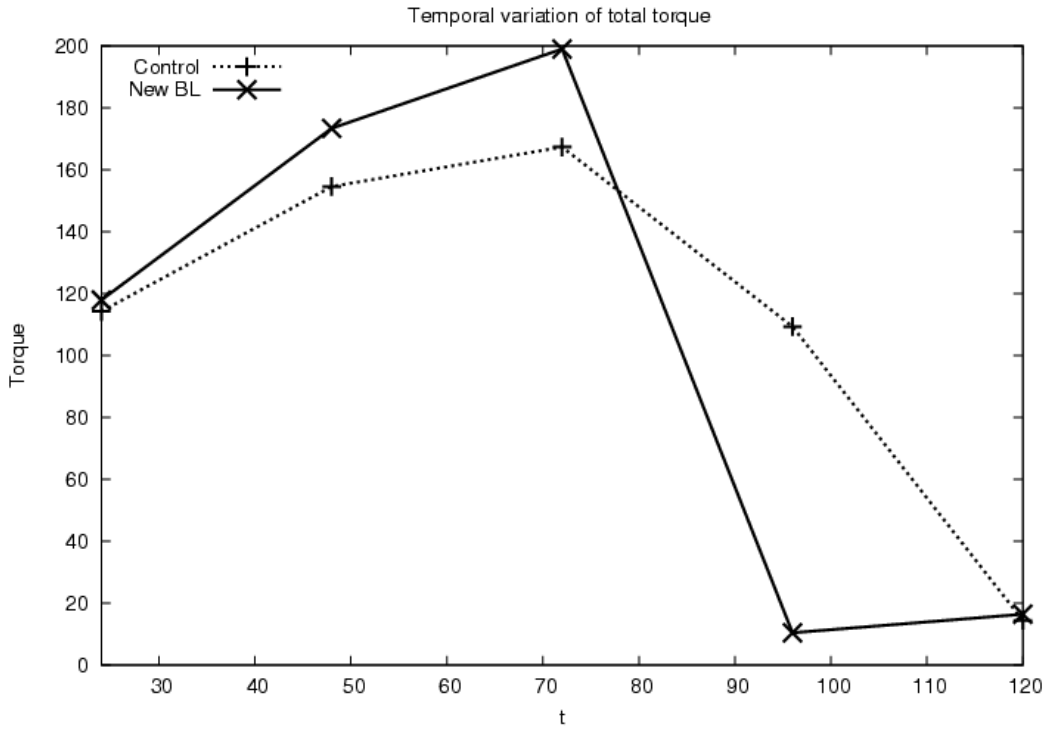

Figure 8: Comparison of the total surface torque (units of N-r*) on the cyclone as a function of time (hours)

4.4 Role played by the BL on intensity prediction

The variation of the simulated intensity of the cyclone in time, as indicated by the minimum sea level pressure, is shown in table 1 and figure 9. In the observations, the storm had achieved the lowest central pressure of 912 hPa on 26 October 1800 UTC, whereas in our simulation, the lowest pressure of only 987 hPa is seen at 60 h (28 October 1200 UTC). This may be attributed to the inadequate horizontal resolution, of about 78 km used in the model. The model resolution is considered fairly coarse particularly for tropical cyclone intensity simulation. Though regional models such as MM5 can be integrated with very high resolution, they suffer from the disadvantage that the lateral boundary conditions must be obtained from a global model. Our model though being a coarser resolution global model, does not suffer from the limitation of lateral boundary conditions.

One can see from figure 9 that for the lower resolution runs, the new boundary layer module increases the simulated pressure drop only by about 2.5 hPa. For the higher resolution, this change is more pronounced: a drop of around 5 hPa at 72 hours, giving a minimum sea-level pressure of 988 hPa during its life on 28 October 1200 UTC. As was the case with the track simulations, the best results are obtained with the new boundary layer at a higher resolution, though no great reduction in the central pressure is achieved. However, the improvement in the central pressure drop using the new boundary layer with a higher resolution is in the right direction. Lower intensity of the cyclone, besides depending on the coarse resolution in our study, may also stem from the inadequacy of the Kuo-Anthes scheme for tropical cyclone intensity simulations.

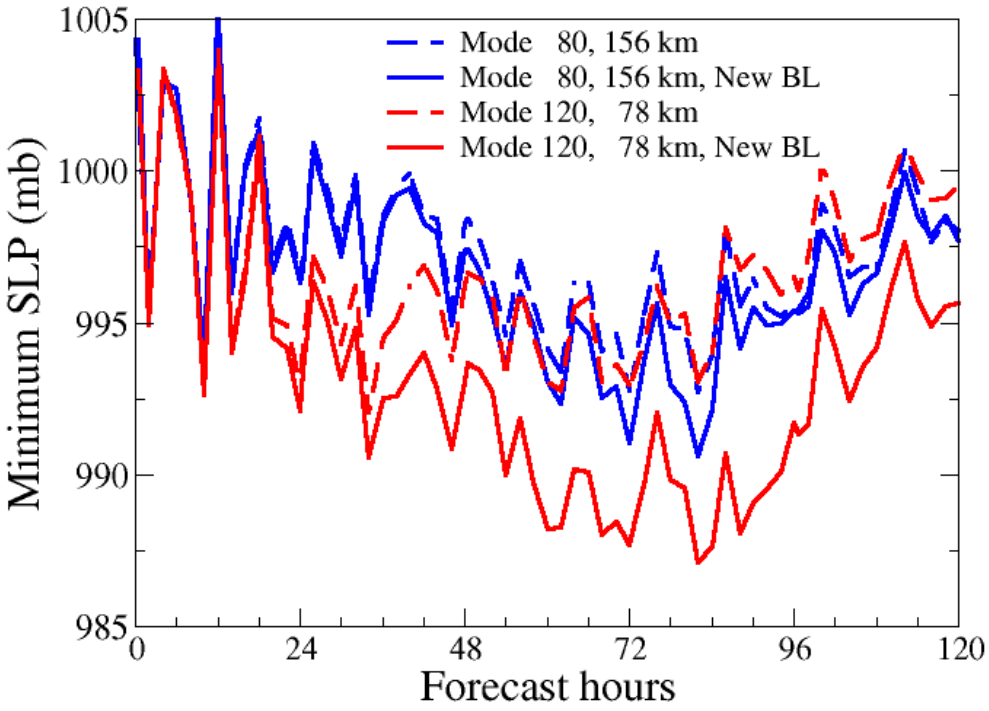

Figure 9: Variation of the minimum sea level pressure as a function of time. The curves corresponding to the control run are shown by dashed lines and for new boundary layer with V_m of 5 m/s by full lines. The 80 mode results are coloured blue and the 120 mode results are coloured red.

5 Discussion and conclusion

We have presented results here on the simulation of the Orissa supercyclone of 1999 using a new GCM called Varsha 1.0 at T-80 and T-120 resolutions.

We make a control run based on the extant T-80 version of the code, and several simulations when the boundary layer module of the control version is replaced by a new module that employs the scaling arguments of Rao and Narasimha (2005). With an improvement in resolution corresponding to T-120, and the new boundary layer module, errors in cyclone track prediction are significantly reduced, to a maximum of about 230 km at 36 h after initialization to about 34 km at 48 h. The lowest error close to landfall is about 55 km at 96 h. However, not much improvement in the pressure drop at the centre has been achieved. This may be due to the Kuo-Anthes cumulus parameterization scheme used in our model. In other simulations being reported in this volume by other groups also, Kuo-Anthes scheme has not produced any significant intensification.

A preliminary analysis of how the new boundary layer code may have effected such an improvement in track prediction is then undertaken. This is an interesting and important issue, as the primary role of the new boundary layer code is to change the parameterization

of low-wind fluxes, whereas the cyclone is usually associated with high winds. The analysis reveals that the total surface force acting on the cyclone mass as a result of surface drag is often substantially higher according to the new boundary layer code (factor of 2.5 at 72 h, for example). Furthermore the direction of this force is such as to push the cyclone towards the observed track. Comparison with the control run also reveals that with the new code the cyclone is more compact, i. e. is a tighter spiral. This effect is here traced to the total surface torque acting on the cyclone. The major contributions to this torque come from two related sources. First, in the outer regions of the cyclone, the active area and moment arm for the stress force are both higher, and the surface stresses from the new code are substantially higher than those in the control run. The net result is that the radial distribution of the torque at 72 h shows a value 40 % higher than that of the control run at a radius $r^* = 5$. At 96 h the torque from the new code falls to a lower value than that in the control run. But much of the contribution to the higher surface forces and torque also come from areas nearer the centre of the cyclone, where the winds are actually higher than in the control run. Clearly, some complex interactions, still to be elucidated, are at work here.

More detailed studies will be required to provide complete explanations of the performance of the new code. At the present stage we can only say that the results are encouraging, and that a preliminary analysis indicates that the new code results in higher surface forces and torque that are qualitatively consistent with the considerably improved track prediction resulting from the code. Also use of other cumulus parameterizations, found to be better for intensity prediction in other NWP models as reported in this volume, within the GCM may prove to be beneficial.

Acknowledgments

The authors would like to acknowledge the financial support received under the NMITLI programme as part of which this work was carried out. The assistance rendered by Sunayan Bandhopadhyay, Bhagyalakshmi K., Sreelekha C. K., Amit K. Verma, and Resmi K. L. of Flosolver Unit, NAL is gratefully acknowledged. We thank Dr. D. R. Sikka for useful comments on the first draft of the manuscript.

References

Emanuel, K. A., 1999, "Thermodynamic control of hurricane intensity." *Nature* **41**, 665 – 669.

Gross, J. M., 2001, "2000 National Hurricane Center Forecast Verification." Web page: www.nhc.noaa.gov/ver00.html.

Hack, J. J., Boville, B. A., Briegleb, B. P., Kiehl, J. T., Rasch, P. J. and Williamson, D. L., 1993, "Description of the NCAR Community Climate Model (CCM2)." NCAR Tech. Note, NCAR/TN-382+STR, NTIS PB93-221802/AS. Climate and Global Dynamics Division, National Center for Atmospheric Research, Boulder, Colorado.

MM5 Community Model. Web page: www.mmm.ucar.edu/mm5.

Nanjundiah, R. S., and Sinha, U. N., 1999, "Impact of Modern Software Engineering Practices on the Capabilities of an Atmospheric General Circulation Model." *Current Science*, **76**, 1114–1116.

Rao, K. G. and Narasimha, R., 2005, "Heat-flux scaling for weakly forced turbulent convection in the atmosphere." *Journal of Fluid Mechanics* (2005).

Sinha, U. N., Sarasamma, V. R., Rajalakshmy, S., Subramanian, K. R., Bharadwaj, P. V. R., Chandrashekar, C. S., Venkatesh, T. N., Sunder, R., Basu, B. K., Sulochana Gadgil, and Raju, A., 1994, "Monsoon forecasting on parallel computers." *Current Science*, **67**, No. 3, 178–184.

Sinha, U. N., Venkatesh, T. N., Mudkavi, V. Y., Vasudeva Murthy, A. S., Nanjundiah, R. S., Sarasamma, V. R., Rajalakshmy S., Bhagyalakshmi K., Verma, A. K., Sreelekha, C. K., and Resmi K. L., 2005, "Comprehensive report on the meteorological aspects of the NMITLI project on Mesoscale modelling for monsoon related predictions." PD FS 0514, National Aerospace Laboratories, Bangalore, India (2005)

Sinha, U. N., Venkatesh, T. N., Sarasamma, V. R., Rajalakshmy S., Bhagyalakshmi K., Verma, A. K., Sreelekha C. K., and Resmi K. L., 2005, "NMITLI GCM code: Varsha 1.0", PD FS 0516, National Aerospace Laboratories, Bangalore, India,

Varghese S., Vasudeva Murthy, A. S., and Narasimha, R., 2003, "A Fast, Accurate Method of Computing Near-Surface Longwave Fluxes and Cooling Rates in the Atmosphere." *Journal of the Atmospheric Sciences*, **60**, 2869–2886.